



Particle size fractionation and chemical speciation of REE in a lateritic weathering profile in Western Australia

Introduction

Physical and chemical weathering of rocks and minerals leads to soil formation. During this processes, mineral transformations result in a mass flux change of elements within the mineral assemblage and among particle size fractions, which yields information on element partitioning and transportation within a profile. The concentration of metals in soils increases with decreasing particle size (Al-Rajhi et al. 1996; Ljung et al. 2006; Acosta et al. 2009) because fine particles usually have a larger specific surface area capable of retaining higher amounts of metals (Wang et al. 2006), or alternatively, metals are co-precipitated with fine-grained secondary minerals. In the course of weathering, weathered regolith shifting into smaller particle sizes can result in the relative accumulation of the REE as refractory elements (Caspari et al. 2006).

However, the substantial influence that the particle size exerts on the abundance and redistribution of REE in lateritic regolith is not well known. Most of the studies on the geochemical behavior of REE during supergene weathering concentrate on bulk regolith. Therefore, a systematic understanding of the occurrence of REE in different grain size fractions of lateritic regolith is needed. Understanding grain size effects would assist pedological interpretation of the fate of REE, and assessment of plant availability of REE under natural environmental conditions.

Currently, in uncontaminated soils, two different approaches for determining trace element location and associated phases are used: physical fractionation and chemical methods (especially sequential selective extraction). Although the sequential extraction method suffers from relying on operationally defined fractions, lack of selectivity for the potential for trace element redistribution and re-adsorption among phases during extraction, it is still considered useful for investigation of associated phases of trace metals in soils by many research workers (e.g. Cao et al. 2000; Aubert et al. 2004). The reactivity or mobility of REE largely depends on their chemical speciation in weathered profiles, however, few studies have dealt with the speciation of REE in non-contaminated soils (Aubert et al. 2004), especially in natural weathered profiles.

continued on page 2

Note: This EXPLORE article has been extracted from the original EXPLORE Newsletter. Therefore, page numbers may not be continuous and any advertisement has been masked.

Particle size fractionation and chemical speciation of REE...

continued from page 1

.....

The objective of this study is to determine the distribution and fractionation of REE in various particle size fractions and associated phases. The concentrations of REE in different particle size fractions and extracted phases are quantified and fractionation of REE with respect to those fractions and phases are discussed.

Materials and Methods

Description of the study areas and sampling

The profile studied (JG) is located at the Jarrahdale Railway cutting (32°17'46"S, 116°5'40"E), 45 m from Alcoa Road, 80 km south-east of Perth in the Darling Range, Western Australia, at an average elevation of 270 m above sea level (Fig. 1). The investigated lateritic JG profile is ca. 12 m deep overlying meta-granitoids. The meta-granitoid is intruded by a dark-colored dolerite dyke, which is seen at the base of the cutting by the contrasts in color and texture of the parent rock and weathered products. The profile is clearly zoned and consists of parent meta-granitoids, saprolite, mottled clay, ferruginous mottled zone,

ferruginous duricrust, upper ferruginous zone and horizon A regolith (Fig. 1). The mottled clay is pale white kaolinite-rich, consisting of a lower zone (JG2) at 8.6 m depth and an upper zone (JG3) at 6.5 m depth. The ferruginous duricrust (3 m depth) is gibbsite and goethite rich. The upper ferruginous zone (JG6, 1.5 m depth) is rich in red iron nodules. In contrast, the horizon A regolith (JG7-10, <1 m depth) is gravely sandy soil rich in dark brown to black loose nodules. The sampling of the profile was conducted on the 6th August, 2009. Based on the different properties (e.g. texture, color, coarse fragment content), each zone was identified and sampled at the depth given above in a 10×10 cm square and put into a sealed plastic box and transported to the laboratory and air dried.

The lateritic profiles at Jarrahdale are commonly considered to have undergone a long period (ca. 2650 Ma by Brimhall et al. (1994)) of in-situ intense weathering

continued on page 4

Particle size fractionation and chemical speciation of REE...

continued from page 2

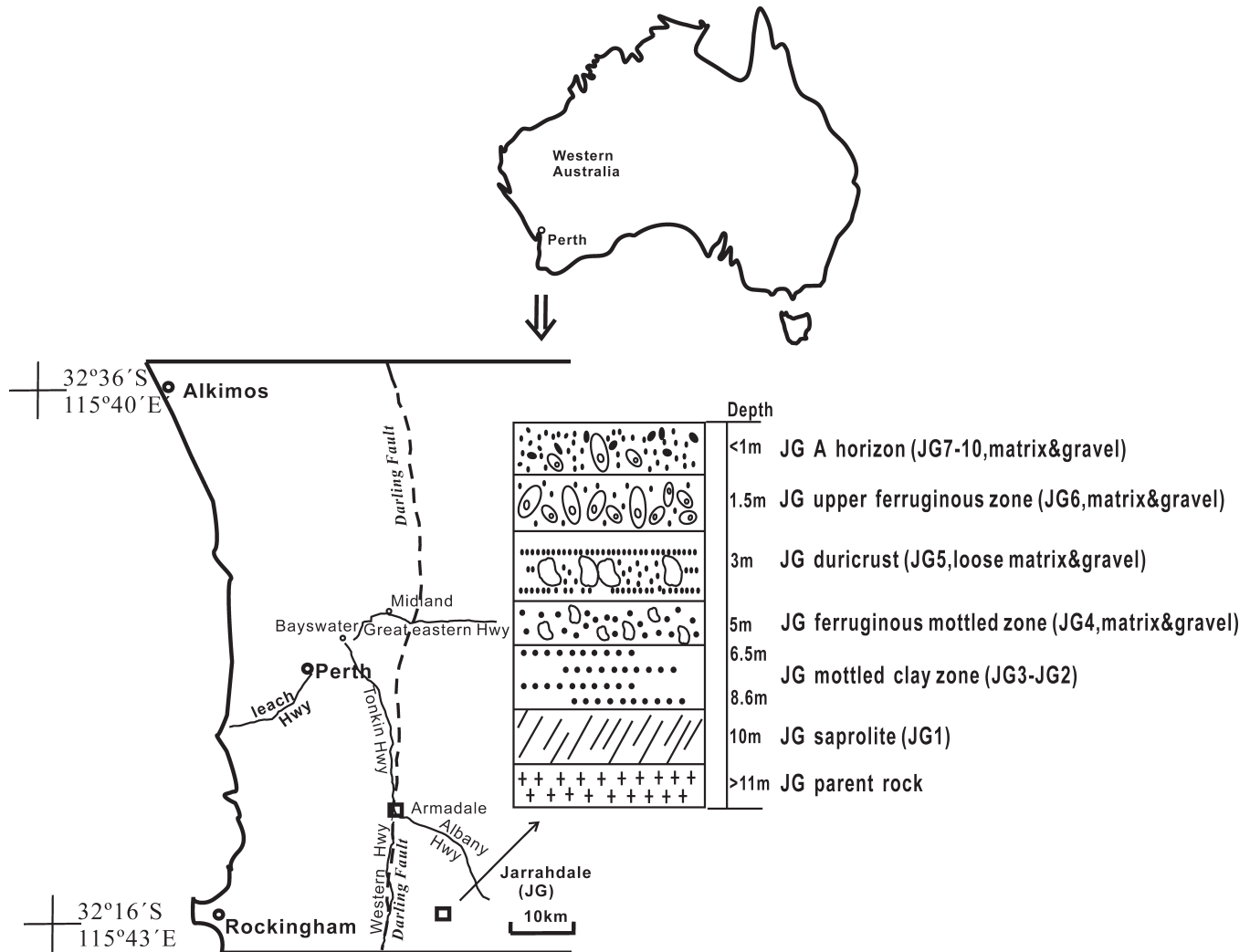


Figure 1 Location of sampling site in Western Australia, showing lateritic regolith profile (JG). The dashed line presents the western margin of the Darling Fault (known as Darling Range, (Gozzard 2007)).

(Sadleir & Gilkes 1976; Anand et al. 1991; Anand & Paine 2002; Anand & Butt 2010). Sadleir & Gilkes (1976) described in detail the lateritic profile at this site and showed significant depletion of Si in the upper part of profile consistent with intense weathering but preservation or enrichment of Al and Fe. The chemical weathering and mineralogy of regolith from lateritic bauxite in the Darling Range have been investigated in a number of studies (e.g. Anand et al. 1991; Anand & Paine 2002; Kew & Gilkes, 2007).

Analytical Methods

Pretreatment of the regolith samples included separation and weighing of each part of soil subsamples into a gravel (>2 mm) fraction, represented by 'g' and matrix (<2 mm) fraction, represented by 'm', with the exception of the mottled clay and saprolite, which have only matrix fractions. The fractions of matrix and gravel were oven dried at 105 °C overnight and ground to ≤ 200 μm prior to fusion in order to determine trace element concentrations. The regolith matrix was further separated into the following three size fractions recommended by the International

Society of Soil Science (ISSS) (Prescott et al. 1934; Marshall 1947, 2003): clay (<2 μm), silt (2-20 μm) and sand (>20 μm) using the sedimentation and wet sieving methods (Day, 1965). Different particle size fractions were rinsed with deionized water three times, oven dried at 105 °C overnight and ground to ≤ 200 μm prior to fusion. The matrix fraction (<2 mm) was used to determine the pH and total carbon (Table 1). Soil pH was determined potentiometrically in the supernatant in a 1:5 suspension of soil: deionized water (Rayment & Higginson 1992) and soil total carbon was determined by Elementar (Vario Macro, Hanau, Germany).

To investigate extracted phases and association behavior of trace elements, a sequential extraction procedure was performed. The matrix fraction (< 2 mm) from the saprolite (JG1m), upper mottled clay (JG3m) and ferruginous duricrust (JG5m) were selected. An in-house laboratory reference material was prepared together with selected samples. Regolith trace elements were extracted as five species (modified from Hall et al. 1996): (a) water soluble, adsorbed, and exchangeable and carbonates bound

continued on page 5

Particle size fractionation and chemical speciation of REE...

continued from page 4

Table 1 Selected properties of regolith matrix fraction (< 2 mm) from the JG profile.

Sample	Depth (m)	soil pH ¹ (H ₂ O)	clay% < 2 μm	silt% 2-20 μm	sand% > 20 μm	TC ² %	Description
JG7	0.02	5.50	8.4	6.8	84.8	6.06	Horizon A
JG8	0.15	5.59	7.0	6.5	86.4	2.19	Horizon A
JG9	0.3	5.54	5.8	6.3	87.9	1.06	Horizon A
JG10	0.4	5.47	6.8	6.5	86.7	0.73	Horizon A
JG6	1.5	5.60	4.3	2.5	93.2	0.47	Upper ferruginous zone
JG5	3.0	5.08	6.5	3.5	90.0	0.30	Ferruginous duricrust
JG4	5.0	4.90	9.0	7.5	83.5	0.20	Ferruginous mottled zone
JG3	6.5	4.55	28.3	7.3	64.4	0.08	Upper mottled clay
JG2	8.6	3.76	29.6	8.5	61.8	0.17	Lower mottled clay
JG1	10.0	3.34	27.0	15.4	57.7	0.27	Saprolite

¹ pH was determined in a 1:5 suspension of soil: deionized water
²TC refers to total carbon, determined by Elementar, Vario Macro, Hanau, Germany.

Table 2. The residual samples and reference materials were rinsed with deionized water three times and oven dried at 105 °C overnight, then were ground to ≤200 μm prior to fusion.

Trace elements, including REE, in 10% HCl dissolved fusion beads were determined by inductively coupled plasma-mass spectroscopy (ICP-MS) by Genalysis Laboratory Services of Intertek Commodities in Maddington, Western Australia. Certified international standard materials, including stream sediment reference material STSD-2, STSD-4 (Canada Centre for Mineral and

(WAE); (b) organic matter and sulphide bound (Org); (c) amorphous Fe-Mn (hydr) oxide bound (Am); (d) crystalline Fe-Mn (hydr)oxide bound (Cry) and (e) residual phase (Res). Since carbonates were unlikely to be present in the regolith being studied here (Anand & Paine 2002) due to low pH, species WAE is considered to include mainly water soluble, adsorbed or exchangeable elements. Sulphides are also scarce in the lateritic regolith, therefore it is assumed that the Org phase is mainly hosted by organic matter complexes. A brief summary of the method is shown in

Energy Technology, CANMET) and an in-house standard material were prepared in the same way as the routine samples and analyzed together with samples to monitor the accuracy and precision. The variation between tested values and expected values was within 10% of the certified values. The concentrations of REE in different particle size fractions are given in Table 3 with REE chemical species in Table 4.

Polished thin sections of air dried resin-impregnated

continued on page 6

Particle size fractionation and chemical speciation of REE...

continued from page 5

regolith and outcrop samples were prepared and examined using a JEOL JSM-6400 scanning electron microscope (SEM) by means of secondary electron (SE) and backscattering electron (BSE) imaging, equipped with a Link analytic energy dispersive spectrometer (EDS) to determine textures, morphology and phase composition of individual grains at 15kV accelerating voltage with 3 nA beam current. Chemical composition of REE-bearing minerals were analyzed for selected representative mineral grains using a JEOL 8530 electron probe micro-analyzer (EPMA) at 20 kV accelerating voltage and 5

nA beam current. Standard REE-bearing references for microprobe calibration were synthetic glasses 612 from National Institute of Standards and Technology (NIST) and in-house standard synthetic phosphates; standard Brazil monazite was analyzed with samples for cross checking. All microscopy analyses were conducted at the Centre for Microscopy, Characterisation and Analysis (CMCA), University of Western Australia. Detection limits for elements determined by EMPA are listed in Appendix 1.

continued on page 7

Table 2. Sequential extraction procedures of REE in lateritic regolith

Step	Speciation	Reagent
a	water soluble, adsorbed, and exchangeable (WAE)	To 1 g of soil sample, add 20 mL of 1.0M CH ₃ COONa (adjust to pH 5 with CH ₃ COOH), room temperature (25°C), shake 6h, centrifuge for 15min at 3000 rpm; rinse with 5 mL H ₂ O twice, mark 30 mL; repeat.
b	organic matter bound (Org)	Add 40 mL 0.1M Na ₄ P ₂ O ₇ , room temperature (25°C), shake 1h, centrifuge; repeat; rinse with 5 mL H ₂ O twice, mark 50 mL; repeat.
c	amorphous Fe (hydr)oxide bound (Am)	Add 20 mL 0.25M NH ₂ OH·HCl in 0.25M HCl, vortex, water bath at 60°C for 2h, centrifuge; rinse with 5 mL H ₂ O twice, mark 30 mL; repeat.
d	crystalline Fe (hydr)oxide bound (Cry)	Add 30 mL 1.0M NH ₂ OH·HCl in 25%CH ₃ COOH, vortex, water bath at 90°C for 3h, centrifuge; rinse with 10 mL 25% CH ₃ COOH twice, mark 50 mL; repeat.
e	residue (Res)	MilliQ water wash residue three times, oven dry at 60°C. Fuse with 12:22 Norrish flux (Lithium metaborate/ Lithium tetraborate), dilute with 100 mL of 10% HCl.

Table 3

sample

Element concentrations (ppm)

	d.l.	Element concentrations (ppm)														
		La	Ce	Pr	Nd	Sm	Eu	Gd	Tb	Dy	Ho	Er	Tm	Yb	Lu	Y
	d.l.	0.1	0.1	0.1	0.1	0.1	0.1	0.1	0.1	0.1	0.1	0.1	0.1	0.1	0.1	0.1
Saprolite	JG1sand	0.3	0.6	b.d.	0.3	0.2	b.d.	0.1	b.d.	0.1	b.d.	0.1	b.d.	0.2	b.d.	1.0
	JG1silt	1.3	2.3	0.2	0.9	0.3	b.d.	0.3	b.d.	0.3	b.d.	0.3	b.d.	0.5	0.1	2.2
	JG1clay	1.2	2.0	0.2	0.8	0.2	b.d.	0.1	b.d.	0.1	b.d.	0.1	b.d.	0.2	b.d.	0.8
	JG1matrix	1.3	2.4	0.2	1.1	0.3	0.1	0.3	0.0	0.2	0.0	0.2	0.0	0.3	0.1	1.3
Lower mottled clay	JG2sand	3.4	4.6	0.4	1.0	0.3	b.d.	0.2	b.d.	0.2	b.d.	0.2	b.d.	0.3	b.d.	1.3
	JG2silt	12.3	17.3	1.5	4.1	0.9	0.1	0.8	0.1	0.8	0.2	0.7	0.1	1.0	0.2	5.6
	JG2clay	9.1	12.1	1.0	2.4	0.4	b.d.	0.3	b.d.	0.3	b.d.	0.2	b.d.	0.3	b.d.	1.6
	JG2matrix	5.2	7.5	0.6	1.7	0.3	0.1	0.2	0.1	0.3	0.1	0.3	0.1	0.5	0.1	2.1
Upper mottled clay	JG3sand	7.0	9.9	1.0	2.5	0.4	b.d.	0.3	b.d.	0.4	0.1	0.4	b.d.	0.7	0.2	2.9
	JG3silt	27.0	38.2	3.5	9.7	1.7	0.3	1.2	0.2	1.4	0.4	1.1	0.2	1.7	0.3	10.2
	JG3clay	22.6	30.2	2.8	7.7	1.1	0.2	0.8	0.1	0.8	0.2	0.4	b.d.	0.5	0.1	4.0
	JG3matrix	10.5	14.8	1.3	3.6	0.6	0.1	0.5	0.1	0.4	0.1	0.3	0.1	0.4	0.1	2.7
Ferruginous mottled zone	JG4sand	4.5	16.0	0.7	2.0	0.4	b.d.	0.3	b.d.	0.3	b.d.	0.2	b.d.	0.3	b.d.	1.8
	JG4silt	20.2	40.7	3.4	10.8	2.2	0.4	1.7	0.3	1.9	0.5	1.6	0.3	2.2	0.5	12.6
	JG4clay	25.1	40.5	4.6	14.8	2.8	0.5	2.0	0.3	1.7	0.4	1.0	0.2	1.1	0.2	7.8
	JG4matrix	7.8	19.0	1.1	4.3	0.9	0.1	0.7	0.1	0.7	0.2	0.6	0.1	0.7	0.2	4.5
Duricrust	JG4gravel	5.0	107	0.6	1.9	0.3	0.1	0.7	0.0	0.4	0.1	0.2	0.0	0.4	0.1	2.1
	JG5sand	5.7	35.8	0.8	2.4	0.5	b.d.	0.4	b.d.	0.5	b.d.	0.3	b.d.	0.4	b.d.	2.5
	JG5silt	13.8	61.1	2.4	7.7	1.6	0.3	1.1	0.2	1.2	0.3	0.9	0.2	1.2	0.2	7.3
	JG5clay	14.9	63.2	2.9	10.1	2.1	0.4	1.5	0.2	1.3	0.3	0.8	0.1	1.0	0.2	5.8
Upper ferruginous zone	JG5matrix	6.1	37.2	0.9	3.0	0.6	0.1	0.7	0.1	0.5	0.1	0.3	0.1	0.5	0.1	3.2
	JG5gravel	6.0	224	0.7	2.4	0.4	0.1	1.6	0.1	0.4	0.1	0.2	0.0	0.3	0.1	2.0
	JG6sand	7.2	21.9	1.5	5.0	1.1	0.2	1.0	0.2	1.1	0.3	0.8	0.1	0.9	0.2	6.8
	JG6silt	14.6	60.1	3.1	10.3	2.0	0.3	1.8	0.3	2.0	0.5	1.5	0.3	1.8	0.4	13.1
Meta-granitoids	JG6clay	17.2	121	4.3	14.8	2.9	0.6	2.5	0.4	2.2	0.5	1.3	0.2	1.2	0.2	13.1
	JG6matrix	7.8	28.8	1.6	5.7	1.1	0.2	1.3	0.2	1.2	0.3	0.9	0.2	1.1	0.2	7.6
	JG6gravel	7.5	27.0	1.7	6.5	1.4	0.3	1.4	0.2	1.4	0.3	0.9	0.2	1.0	0.2	5.3
	Average PR	27.9	47.4	4.3	14.0	2.1	0.5	1.8	0.2	1.0	0.2	0.8	0.2	1.1	0.2	8.5

Table 3. Concentrations of REE in different particle size fractions in the lateritic JG profile in Western Australia. b.d. refers to values below detection limit; Average PR refers to average value of each REE in parent meta-granitoids.

Particle size fractionation and chemical speciation of REE...

continued from page 6

$$GSF_{loading} = 100 \times \left(\frac{X_i \times GS_i}{\sum_{i=1}^n X_i \times GS_i} \right)$$

Calculation of mass loading of REE in particle size fraction

To index an element's partitioning into different particle size fractions, a mean element mass loading was calculated based on its concentration in a selected grain size of known mass percent (Sutherland 2003).

Where:

X_i is the concentration of REE (ppm) in an individual grain size fraction (e.g. <2 μ m);

GS_i is the mass percentage of an individual fraction, which has limits of 0-100%.

$GSF_{loading}$ is the element mass loading in a selected grain size and the summation of $GSF_{loading}$ indices for each soil sample equals 100%.

In the ferruginous zone, four classes of particle sizes (clay, silt, sand and gravel) were defined and three in the mottled clay zone and saprolite (clay, silt and sand). Thus, if the REE concentration for a given fraction is very high but it forms only a small portion of the overall sample mass, the contribution of this fraction to the total sample REE loading will be minimal. The mass loading of each fraction of regolith samples are listed in Table 5.

Results**Concentrations of REE in different particle size fractions**

In the lateritic profile studied (JG), silt and clay fractions generally contained the highest concentrations of REE, except in the saprolite (Fig. 2). In the ferruginous zone (from JG6 to JG4, 1.5-5 m depth) clay contained the highest concentrations of LREE (from La to Nd), followed by the silt fraction. In the duricrust (3 m depth) and ferruginous mottled zone (5 m depth), however, gravel was abnormally enriched in Ce. Concentrations of LREE in matrix were slightly higher than in sand in the ferruginous zone. In the mottled clay (6.5-8.6 m depth) and saprolite (10 m depth), the relative concentrations of LREE from high to low were: silt > clay > sand. MREE (from Sm to Ho) had different distribution patterns between the particle size fractions. From Sm to Gd, closer to LREE, the highest concentrations were in the clay fraction in the ferruginous zone but in the silt fraction in the mottled clay zone. From Tb to Ho, closer to HREE, silt fraction had the highest concentrations except the duricrust and upper ferruginous zone. HREE (from Er to Lu) and Y, showed mostly consistent distribution patterns. The silt fraction contained the highest concentration of HREE throughout the profile followed by the clay fraction in the ferruginous zone. In the saprolite and mottled clay, both clay and sand fractions had similar HREE concentrations.

continued on page 8

Sample	Element concentrations (ppm)														
	La	Ce	Pr	Nd	Sm	Eu	Gd	Tb	Dy	Ho	Er	Tm	Yb	Lu	Y
d.l.	0.001	0.001	0.001	0.001	0.001	0.001	0.001	0.001	0.001	0.001	0.001	0.001	0.001	0.001	0.001
JG1_WAE	0.140	0.290	0.040	0.149	0.032	0.007	0.021	0.003	0.017	0.004	0.013	0.002	0.018	0.003	0.055
JG1_Org	0.008	0.009	0.002	0.006	0.003	b.d.	0.001	b.d.	0.002	b.d.	0.001	b.d.	0.002	b.d.	0.007
JG1_Am	0.016	0.032	0.004	0.013	0.004	b.d.	0.003	b.d.	0.003	b.d.	0.002	b.d.	0.003	b.d.	0.016
JG1_Cry	0.023	0.014	0.001	0.003	0.001	b.d.	0.001	b.d.	0.001	b.d.	b.d.	b.d.	0.001	b.d.	0.007
JG1_Res	1.1	1.9	0.2	0.7	0.2	b.d.	0.2	b.d.	0.2	b.d.	0.2	b.d.	0.3	b.d.	1.3
JG3_WAE	0.938	0.905	0.168	0.531	0.083	0.018	0.086	0.014	0.070	0.016	0.041	0.006	0.031	0.005	0.277
JG3_Org	0.022	0.019	0.004	0.013	0.002	b.d.	0.002	b.d.	0.002	b.d.	0.001	b.d.	0.003	b.d.	0.012
JG3_Am	0.130	0.200	0.028	0.098	0.019	0.004	0.018	0.003	0.016	0.003	0.010	0.002	0.009	0.002	0.098
JG3_Cry	0.053	0.079	0.008	0.028	0.005	b.d.	0.004	b.d.	0.004	b.d.	0.002	b.d.	0.002	b.d.	0.023
JG3_Res	9.2	13.0	1.1	2.8	0.5	b.d.	0.3	b.d.	0.3	b.d.	0.2	b.d.	0.4	0.2	2.0
JG5m_WAE	0.422	2.744	0.149	0.586	0.146	0.031	0.102	0.015	0.073	0.014	0.037	0.005	0.030	0.005	0.164
JG5m_Org	0.031	0.563	0.015	0.058	0.014	0.003	0.009	0.001	0.006	0.001	0.005	0.001	0.012	0.003	0.028
JG5m_Am	0.127	2.553	0.054	0.221	0.060	0.012	0.042	0.007	0.038	0.008	0.020	0.003	0.020	0.003	0.108
JG5m_Cry	0.049	1.450	0.011	0.039	0.010	0.002	0.006	0.001	0.007	0.001	0.004	b.d.	0.004	b.d.	0.027
JG5m_Res	6.0	27.1	0.8	2.5	0.5	b.d.	0.3	b.d.	0.4	b.d.	0.3	b.d.	0.4	b.d.	2.4

Table 4. Concentrations of REE in different chemical species of representative regolith in the JG profile in Western Australia. All REE determined in extracted WAE, Org, Am and Cry have 0.001 ppm detection limit whereas in Res (fusion method) have 0.1 ppm detection limit by ICP-MS. b.d. refers to values below detection limit.

Particle size fractionation and chemical speciation of REE...

continued from page 7

Table 5

Sample	Mass loading (%)														
	La	Ce	Pr	Nd	Sm	Eu	Gd	Tb	Dy	Ho	Er	Tm	Yb	Lu	Y
JG1sand	24.9	27.9	n.a.	32.8	53.6	n.a.	44.1	n.a.	44.1	n.a.	44.1	n.a.	46.9	n.a.	51.0
JG1silt	28.7	28.5	36.3	26.2	21.4	n.a.	35.3	n.a.	35.3	n.a.	35.3	n.a.	31.2	n.a.	29.9
JG1clay	46.5	43.5	63.7	40.9	25.0	n.a.	20.6	n.a.	20.6	n.a.	20.6	n.a.	21.9	n.a.	19.1
JG2sand	36.0	36.0	36.8	36.8	48.7	n.a.	44.0	n.a.	44.0	n.a.	51.0	n.a.	51.6	n.a.	45.8
JG2silt	18.0	18.7	19.1	20.8	20.2	n.a.	24.3	n.a.	24.3	n.a.	24.6	n.a.	23.7	n.a.	27.2
JG2clay	46.1	45.3	44.1	42.3	31.1	n.a.	31.6	n.a.	31.6	n.a.	24.4	n.a.	24.7	n.a.	27.0
JG3sand	35.0	36.0	36.9	35.8	37.2	n.a.	38.1	n.a.	44.0	42.9	57.1	n.a.	61.2	72.0	49.5
JG3silt	15.2	15.7	15.3	15.7	17.8	27.8	17.2	33.9	17.4	19.4	17.7	n.a.	18.1	12.2	20.0
JG3clay	49.7	48.3	47.8	48.5	45.0	72.2	44.7	66.1	38.7	37.7	25.1	n.a.	20.7	15.8	30.5
JG4sand	34.6	14.6	34.9	32.7	34.9	n.a.	24.6	n.a.	31.1	n.a.	31.2	n.a.	33.4	n.a.	33.1
JG4silt	14.0	3.3	15.2	15.9	17.3	24.0	12.6	28.6	17.7	30.1	22.4	32.9	22.0	39.0	20.9
JG4clay	20.8	4.0	24.7	26.1	26.3	36.0	17.7	34.3	19.0	28.8	16.8	26.3	13.2	18.7	15.5
JG4gravel	30.6	78.1	25.2	25.3	21.5	40.0	45.1	37.2	32.2	41.1	29.6	40.9	31.3	42.3	30.5
JG5sand	43.0	13.6	44.7	41.8	46.2	n.a.	18.9	n.a.	49.1	n.a.	48.5	n.a.	47.7	n.a.	48.0
JG5silt	4.1	0.9	5.2	5.2	5.8	9.4	2.0	8.1	4.6	11.2	5.7	12.9	5.6	9.3	5.5
JG5clay	8.1	1.7	11.7	12.7	14.0	23.3	5.1	15.0	9.2	20.8	9.4	12.0	8.6	17.4	8.1
JG5gravel	44.8	83.8	38.3	40.3	34.0	67.4	74.0	76.9	37.1	68.0	36.5	75.1	38.2	73.3	38.4
JG6sand	15.9	13.6	14.8	13.2	13.4	12.7	12.4	15.3	13.6	17.1	15.3	11.8	15.0	18.1	20.2
JG6silt	0.9	1.0	0.8	0.7	0.7	0.5	0.6	0.6	0.7	0.8	0.8	0.9	0.8	1.0	1.0
JG6clay	1.7	3.4	1.9	1.8	1.6	1.7	1.4	1.4	1.2	1.3	1.1	1.1	0.9	0.8	1.8
JG6gravel	81.5	81.9	82.5	84.3	84.4	85.1	85.6	82.7	84.5	80.9	82.8	86.2	83.2	80.1	77.0

Table 5. Mass loading of REE in different particle size fractions in a lateritic profile in Western Australia. n.a. refers to not available since the element concentration was below the detection limit.

Mass loading of REE in different particle size fractions

Given the mass percentage of each particle size, the mass loading of selected REE in each particle size fraction was plotted in Fig. 3. Although silt and clay fractions had the highest concentrations of REE, their relatively low mass percentage compared with other fractions minimized the enrichment.

In the ferruginous zone, gravel dominated the distribution and abundance of Ce, with up to 84% Ce in the duricrust. In the upper ferruginous zone (1.5 m depth), gravel and sand accounted for more than 95% mass of REE, decreasing to ca. 80% in duricrust (3 m depth) and ca. 60% in ferruginous mottled zone (5 m depth). In the duricrust, the mass loading of each REE was higher in the clay fraction than the silt fraction. In the ferruginous

mottled zone, however, REE were fractionated; the mass loadings of LREE and MREE were higher in the clay fraction and the mass loading of HREE higher in the silt fraction.

From the upper mottled clay to the saprolite (JG3-JG1, 6.5-10 m depth), the regolith does not contain gravel. The clay fraction was the most important host for LREE in these zones (6.5-10 m depth), especially in the upper mottled clay zone (6.5 m depth) with ca. 48%-50% LREE was in the clay fraction. Higher mass loadings of HREE (44%-61%), however, were found to be in the sand fraction in the saprolite and mottled clay. The mass loading of REE in the silt fraction increased with depth from upper mottled clay to saprolite.

continued on page 9

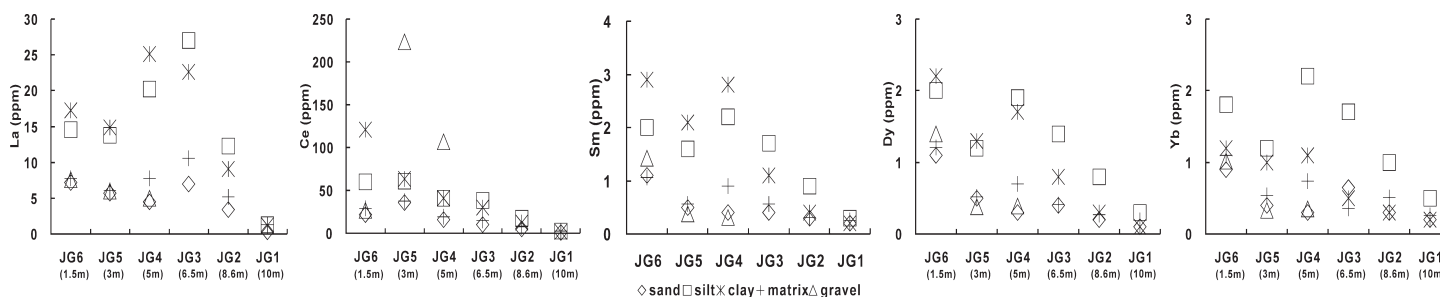


Figure 2. Concentrations of REE in different particle size fractions in the JG profile developed on meta-granitoids in Jarrahdale, Western Australia.

Particle size fractionation and chemical speciation of REE...

continued from page 8

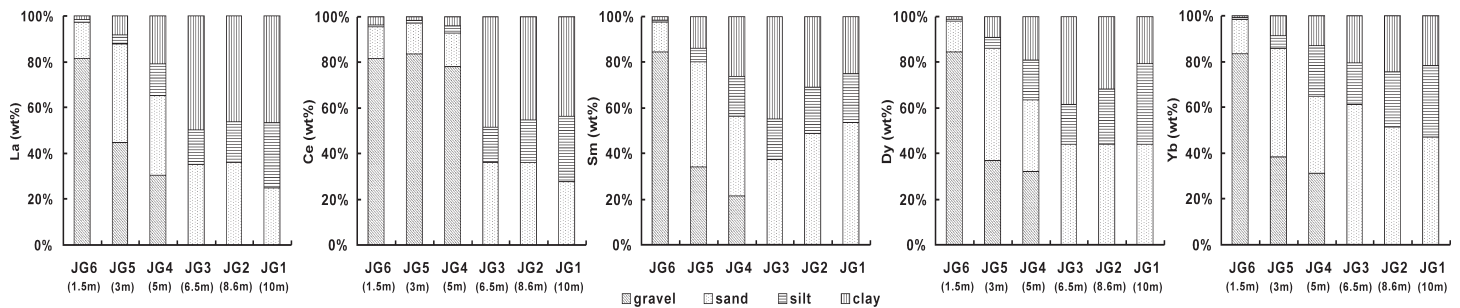


Figure 3. Mass loading of REE in different particle size fractions in the JG profile developed on meta-granitoids in Western Australia (JG6-upper ferruginous zone, 1.5 m depth; JG5-ferruginous duricrust, 3 m depth; JG4-ferruginous mottled zone, 5 m depth; JG3-upper mottled clay, 6.5 m depth; JG2-lower mottled clay zone, 8.6 m depth; JG1-saprolite, 10 m depth. Only selected REE are plotted here; other REE showed similar patterns).

Speciation of REE from sequential extraction

The sequential extraction experiment revealed the percentages of total REE in each chemical phase of representative lateritic regolith in the JG profile (Fig. 4.) Generally, the total REE distribution percentage followed the order: Res > WAE > Am > Cry and Org. The Res and WAE phases dominated the distribution and abundance of REE, accounting for 89%-98% LREE, 87%-97% MREE and 91%-98% HREE. The saprolite Res had higher percentages of MREE (85%) and HREE (92%) than the upper mottled clay (75% MREE and 88% HREE) and duricrust (66% MREE and 82% HREE) and the percentages decreased from saprolite to duricrust. In addition, the saprolite WAE had higher percentage of LREE (13%) than the upper mottled clay (9%) and duricrust (9%). The percentages of MREE (12%) and HREE (7%) in saprolite WAE were lower than in the WAE of the upper mottled clay (20% MREE and 9% HREE) and duricrust (21% MREE and 9% HREE).

The duricrust Org had higher percentage of total REE (1.5%) than the Org in the saprolite (0.6%) and upper mottled clay (0.2%). The percentages of total REE hosted in the Am phase of the duricrust (6.6%) were also higher than in the Am phases of the saprolite (1.4%) and upper mottled clay (1.7%). Similarly, the Cry phase in the duricrust also had higher percentages of total REE (3.3%) than the total REE percentage in the Cry of saprolite

(0.8%) and upper mottled clay (0.6%). In addition, in the duricrust the percentage of REE in the Am phase (6.6%) was higher than the percentages of REE in the Cry (3.3%) and Org (1.5%) phases.

Discussion

Although sequential extraction schemes do not extract chemically discrete forms of elements, the data have revealed variation of the REE distribution in different particle size fractions and extracted phases. Most of REE were hosted by the residual phase, indicating that both the abundance and distribution of REE are controlled by mineral phases in intensely weathered regolith. SEM imaging and EPMA analyses show that LREE are mostly hosted by secondary phosphates ca. 2-20 μm -size, e.g. rhabdophane and florencite, and HREE are mainly contained in weathering-resistant minerals of varied grain size (1-100 μm), e.g. xenotime, zircon and anatase in the lateritic regolith (Fig. 5). The high concentration of REE in the silt fraction (2-20 μm) is in good agreement with the REE-bearing mineral size in the regolith, especially LREE-rich secondary minerals, indicating morphological and mineralogical change from REE-bearing accessory minerals e.g. apatite, fluorocarbonates and thorite in the parent meta-granitoids to secondary rhabdophane and florencite during intense weathering and lateritization (Fig. 5, Table

continued on page 10

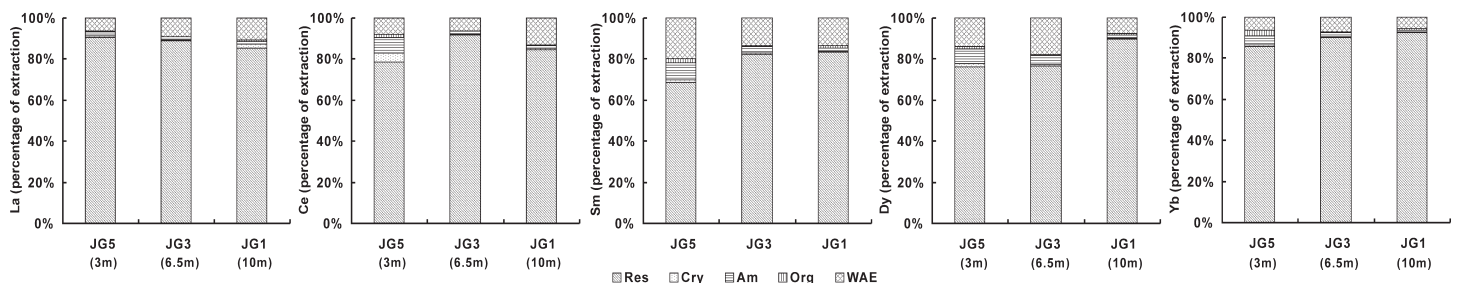


Figure 4. Distribution of total REE among five sequential species of representative JG regolith. (Res: residual; Cry: crystalline Fe (hydr)oxides; Am: amorphous Fe (hydr)oxides; Org: organic matter; WAE: water soluble, adsorbed and exchangeable. JG5-ferruginous duricrust, 3 m depth; JG3-upper mottled clay, 6.5 m depth; JG1-saprolite, 10 m depth. (Some REE concentrations were below the detection limit of ICP-MS and are not presented here).

Particle size fractionation and chemical speciation of REE...

continued from page 9

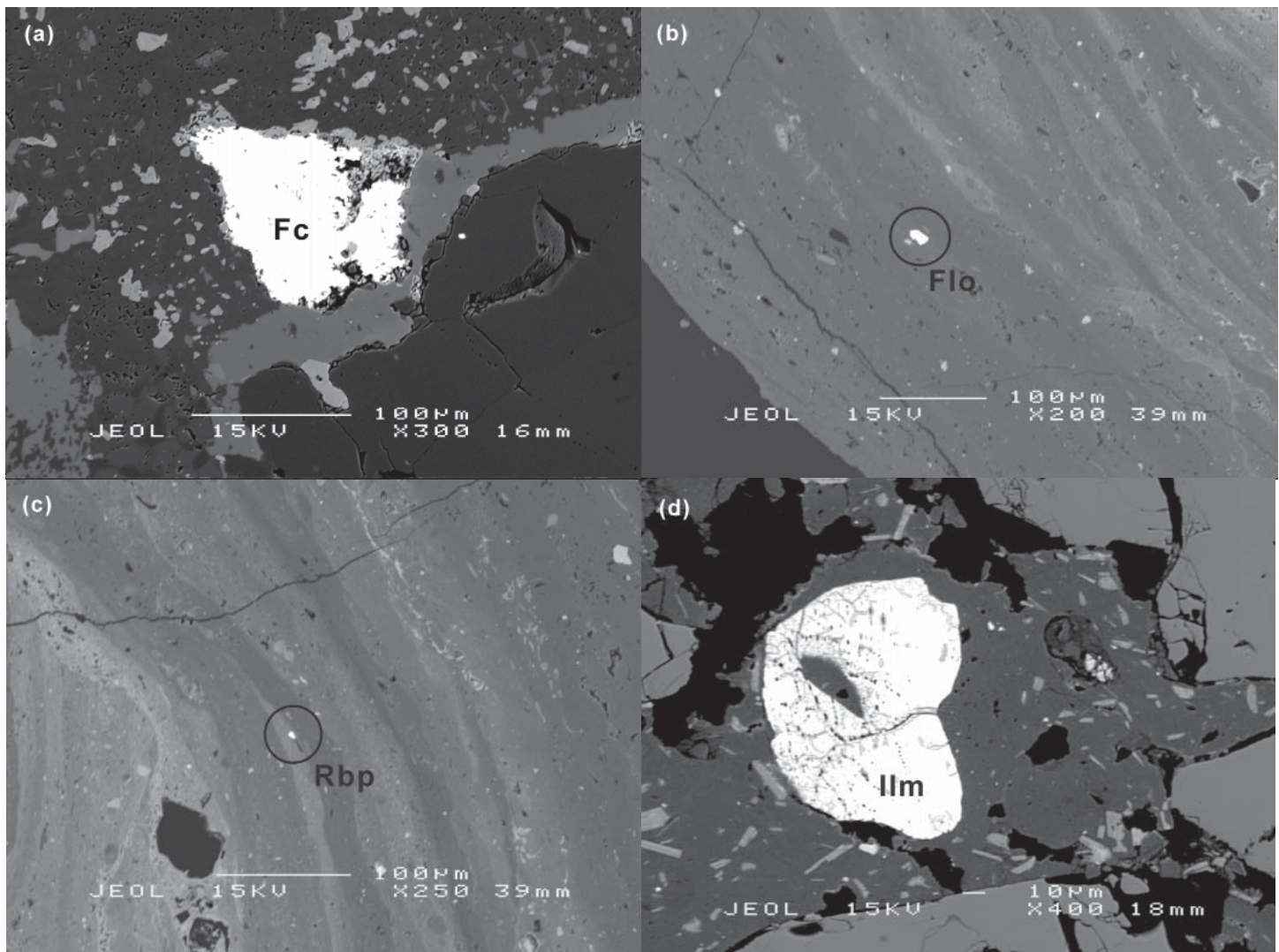


Figure 5. REE-bearing minerals in weathered lateritic regolith of JG profile: (a) fluorocarbonate in parent meta-granitoids; (b) and (c) secondary minute grains of florencite and rhabdophane respectively in ferruginous nodules; (d) ilmenite with REE in ferruginous mottled zone (elemental analyses of these minerals are listed in Table 6; Fc: REE-rich fluorocarbonate; Flo: florencite; Rbp: rhabdophane; Ilm: ilmenite).

Table 6

Sample Element concentrations (wt%)

Sample	Si	Ti	Pb	Th	U	Al	Y	La	Ce	Pr	Nd	Sm	Eu	Gd	Dy	Yb	Lu	Fe	Mg	Ca	P	S	F	O	total
a	2.2	0.03	0.23	0.64	0.18	0.44	0.06	20.8	27.7	2.85	5.97	0.52	0.06	0.27	b.d.	b.d.	b.d.	2.96	0.15	2.89	0.02	0.29	6.31	12.9	87.5
b	0.46	0.06	0.13	3.05	0.02	18.5	0.23	8.19	16.8	1.90	1.74	0.59	0.16	0.48	0.04	0.14	b.d.	0.47	b.d.	0.05	7.71	0.06	0.65	31.3	92.1
c	0.08	0.04	0.54	3.93	0.9	b.d.	1.61	11.8	23.2	2.55	9.07	1.58	0.21	1.05	0.45	0.35	0.03	0.45	b.d.	0.24	12.9	b.d.	0.91	26.3	98.3
d	b.d.	31.9	b.d.	b.d.	0.02	b.d.	b.d.	b.d.	b.d.	b.d.	b.d.	b.d.	b.d.	b.d.	2.18	b.d.	b.d.	27.7	0.06	b.d.	b.d.	b.d.	b.d.	29.7	91.5

Table 6. Concentrations of REE and other elements in mineral phases in parent meta-granitoids and lateritic regolith of a profile in Western Australia, based on electron microprobe spot analyses. Concentrations of Ho, Er, Tm and Tb are below detection limits (b.d.). a, b, c and d represent minerals in Figure 5. a, fluorocarbonate; b, florencite; c, rhabdophane; d, ilmenite.

continued on page 11

Particle size fractionation and chemical speciation of REE...

continued from page 10

6). In addition, in the duricrust an abnormal enrichment of Ce was observed, especially in gravel. It suggests that Ce fractionated from other LREE and less likely to be mobile than the other REE during formation of duricrust and iron nodules. This agrees with high percentages of Ce in the Am and Cry extracted phases in the duricrust.

A significant proportion of REE bound to the WAE phase in natural uncontaminated soils is not common in previous studies and may suggest that a large amount of REE is bio-available in the regolith studied here. High deficiency of REE in the profile, especially in the saprolite, may be partially attributed to low soil pH which favors the conversion of metals from precipitated forms into dissolved forms (Harter 1983; Cao et al. 2001). In an acidic environment, such as this (pH ranges from 3.3 to 4.5 from

saprolite to mottled clay), the predominant REE phase in solution is the free Ln³⁺ ion (Ln denotes REE). In the duricrust, REE may also partially occur as LnHCO₃²⁺ complexes due to the slightly higher pH (5.1) and organic REE complexes due to relatively higher dissolved organic matter (total carbon 0.30%) than in the mottled clay below (total carbon 0.08%). Extraction of adsorbed or exchangeable REE in a spodosol profile has been reported to be closely related to pH, in the range 4.2 to 6.5 (Land et al. 1999).

In addition, the high proportion of REE bound to the WAE is probably relevant to high concentrations of REE in the clay fraction. Kaolinite and halloysite were identified in the saprolite and mottled clay. The transformation from kaolinite to halloysite during weathering is accompanied

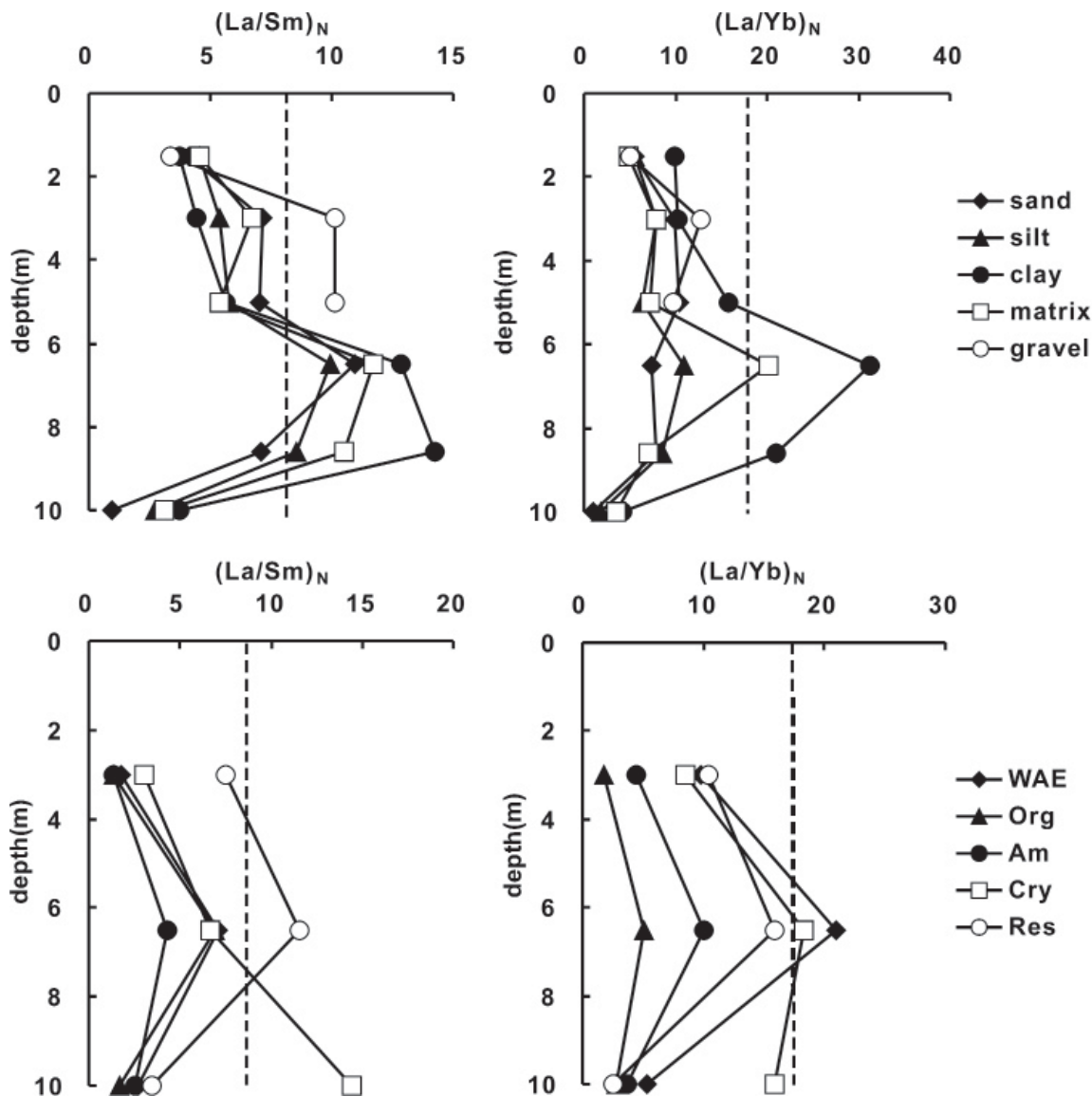


Figure 6. Normalized ratios of (La/Sm)_N and (La/Yb)_N in particle size fractions and sequential extracts in the JG profile developed on meta-granitoids in Western Australia (solid vertical lines are the normalized ratios of average parent meta-granitoids; average chondrite values were used as the reference (Anders & Grevesse 1989))

Particle size fractionation and chemical speciation of REE...

continued from page 11

by an increase in hydration, a decrease in Si/Al ratio and an increasing cation exchange capacity (CEC) (Tari et al. 1999). The clay sized fraction of mottled clay had higher (La/Sm)N (12.9-14.3) and (La/Yb)N (21.0-31.3), compared with (La/Sm)N = 8.4 and (La/Yb)N = 17.5 of averaged meta-granitoids (Fig. 6). Chondrite values were used for REE normalization (Anders & Grevesse 1989). These higher ratios of LREE/MREE and LREE/HREE suggest that clay acts an important role in trapping REE, especially LREE. This is also supported by Cullers et al. (1987) who showed that heavy minerals (biotite, hornblende and sphene) in a soil developed from a granitic parent material appeared to be altering and making LREE available to the clay minerals forming in the soil. However, opposite fractionation (HREE more sorbed than LREE) onto kaolinite has also been reported (Coppin et al. 2002). Adsorption of REE by clay is controlled by the nature of the clay minerals, pH, ionic strength, the presence of additional ligands such as carbonate or organic complexes, surface coverage, and effects specific to the characteristics of the different REE (Koeppenkastrop & Decarlo 1992, 1993; Fendorf & Fendorf 1996; Coppin et al. 2002; Piasecki & Sverjensky 2008; Laveuf & Cornu 2009). As well as these controls, differences in clay mineralogy can affect fractionation of REE (Laveuf & Cornu 2009), potentially explaining the contradictory signatures of REE adsorbed by clay minerals. Usually, REE adsorption increases with increasing pH (Coppin et al. 2002), which may explain the increasing concentrations of REE in the WAE and clay fraction from saprolite to duricrust. The lowest values of (La/Sm)N (0.9) and (La/Yb)N (1.0) in the saprolite sand suggest that La was substantially fractionated from Sm and Yb and greatly depleted from the saprolite, especially in the sand fraction. It is probable that LREE-rich accessory minerals (e.g. fluorocarbonates and thorite), with grain sizes ca. 100 μm , in parent meta-granitoids break down at the initial stage of weathering. In addition, a high mass of HREE is observed in sand from saprolite to upper mottled clay, in contrast to most of LREE being present in clay in these zones. This may suggest that relatively large-grained (ca. 100 μm) and weathering-resistant minerals, e.g. zircon, anatase or ilmenite contained significant amounts of HREE, or, alternatively, HREE may be adsorbed onto larger-grained metal-oxide surfaces, e.g. rutile, hematite (Piasecki & Sverjensky 2008).

The Am and Cry had higher percentages of LREE and MREE than HREE throughout the regolith studied. In the duricrust the Am phase had a preference for MREE whereas the Cry showed a preference for LREE. Since there are negligible variations in complexation constants for the acetate ligand with various REE (Wood 1993), the fractionation in extraction of the Cry is not caused by the extractant solution (Land et al. 1999) in which the only other solute is $\text{NH}_2\text{OH}\cdot\text{HCl}$. The reasons why Am and Cry phases show different preferences for LREE and MREE is not clear, but are believed to be related to pH and the presence of other ligands such as organic complexes (Quinn

et al. 2006; Piasecki & Sverjensky 2008). The fractionation between LREE, MREE and HREE in Fe- (hydr)oxides is subject to debate (Laveuf & Cornu 2009) and varied fractionation with enrichments of LREE (Koeppenkastrop & Decarlo 1993), MREE (Bau 1999; Land et al. 1999) or HREE (Elderfield & Greaves 1981; Marker & Deoliveira 1994) have been observed. For example, Land et al. (1999), studying a spodosol profile, observed an enrichment of MREE in the Am and a clear HREE enrichment relative to the LREE in Cry and Org phases. The differences in REE fractionation between extracted phases probably also arise from the various proportions of the different types of Fe- and Mn oxides present (Laveuf & Cornu 2009). The affinity of Ce with Fe (hydr)oxides indicates surface sorption and oxidation/coprecipitation of Ce onto Fe (hydr)oxides, which have been examined by many authors (Davranche et al. 2004; Bau & Koschinsky 2009; Nedel et al. 2010). The Org phase plays an important role in complexing HREE in this study, especially in the duricrust in contrast to the Am which have a preference for MREE. Affinity of HREE for organic materials has been observed before (Land et al. 1999; Aubert et al. 2004). Organic ligands form complexes with HREE which are more stable than those with LREE (Henderson, 1984; Sonke & Salters, 2006). The proportion of total REE hosted by the Am is higher than both Org and Cry phases, indicating amorphous Fe (hydr)oxide plays a more important role than other solid components in controlling the mobility and bioavailability of REE in lateritic regolith.

Conclusions

A systematic study of particle size fractionation and chemical fractionation of REE in a lateritic weathered profile developed on meta-granitoids in Jarrahdale, Western Australia showed that most of the REE (by mass) had partitioned into coarse-grained material (gravel and sand), despite the high concentrations in fine-grained (silt and clay) fractions. This partitioning by grain size was not consistent, however, across the REE series, with significant fractionation occurring. For example, in the lower profile most LREE mass was in the clay (<2 μm) fraction, but most HREE were associated with sand (>20 μm). The most significant fractionation of REE was shown by a strong Ce anomaly in ferruginous duricrust, consistent with formation of both ferruginous materials and the Ce enrichment by oxidative processes such as precipitation of ferric minerals. Particle size, sequential extraction, and electron microprobe data were consistent with REE occurrence being dominated, in intensely weathered regolith, by mineral phases resistant to weathering. The dominance of residual forms in sequential extracts supported this conclusion, but the existence of significant REE in water soluble, exchangeable or adsorbed forms was surprising and was likely to be related to the low pH of regolith materials. This study demonstrates that the distribution and fractionation of REE within different particle size

continued on page 13

Particle size fractionation and chemical speciation of REE...

continued from page 12

fractions and chemically extractable species can be used as clues for better understanding geochemical behavior of REE in intensely weathered lateritic profiles. Both have potential implication for pedological interpretation of the fractionation of REE during weathering and lateritization, especially when a particle size sorting process is involved.

Acknowledgements

This work was financially supported by the Association of Applied Geochemists (AAG) through its Student In-kind Support Grant, the University of Western Australia and the China Scholarship Council. We are thankful to R. Pearce, T. Quinn and M. Smirk for their analytical expertise. We also thank P. Duncan, J. R. Muhling, and D. Adams of the Centre for Microscopy, Characterisation and Analysis (CMCA) for microscopy and microanalysis. Special thanks are addressed to E. Weiland and J. Flynn for coordination the analyses. Ryan Noble is thanked for his constructive comments of the manuscript. The manuscript has been benefited from the editorial guidance of B. McClenaghan.

References

- ACOSTA, J. A., CANO, A. F., AROCENA, J. M., DEBELA, F. & MARTÍNEZ-MARTÍNEZ, S. 2009. Distribution of metals in soil particle size fractions and its implication to risk assessment of playgrounds in Murcia City (Spain). *Geoderma*, 149, 101-109.
- AL-RAJHI, M. A., ALSHAYEB, S. M., SEAWARD, M. R. D. & EDWARDS, H. G. M. 1996. Particle size effect for metal pollution analysis of atmospherically deposited dust. *Atmospheric Environment*, 30, 145-153.
- ANAND, R. R., GILKES, R. J. & ROACH, G. I. D. 1991. Geochemical and mineralogical characteristics of bauxites, Darling Range, Western Australia. *Applied Geochemistry*, 6, 233-248.
- ANAND, R. R. & PAINE, M. 2002. Regolith geology of the Yilgarn Craton, Western Australia: implications for exploration. *Australian Journal of Earth Sciences*, 49, 3-162.
- ANAND, R. R. & BUTT, C. R. M. 2010. A guide for mineral exploration through the regolith in the Yilgarn Craton, Western Australia. *Australian Journal of Earth Sciences*, 57, 1015-1114.
- ANDERS, E. & GREVESSE, N. 1989. Abundances of the elements-meteoritic and solar. *Geochimica et Cosmochimica Acta*, 53, 197-214.
- AUBERT, D., PROBST, A. & STILLE, P. 2004. Distribution and origin of major and trace elements (particularly REE, U and Th) into labile and residual phases in an acid soil profile (Vosges Mountains, France). *Applied Geochemistry*, 19, 899-916.
- BAU, M. 1999. Scavenging of dissolved yttrium and rare earths by precipitating iron oxyhydroxide: Experimental evidence for Ce oxidation, Y-Ho fractionation, and lanthanide tetrad effect. *Geochimica et Cosmochimica Acta*, 63, 67-77.
- BAU, M. & KOSCHINSKY, A. 2009. Oxidative scavenging of cerium on hydrous Fe oxide: Evidence from the distribution of rare earth elements and yttrium between Fe oxides and Mn oxides in hydrogenetic ferromanganese crusts. *Geochemical Journal*, 43, 37-47.
- BRIMHALL, G.H., COMPOSTON, W., WILLIAMS, I.S., REINFRANK, R.F. & LEWIS, C.J. 1994. Darwinian zircons as provenance tracers in dust-size exotic components in laterites: mass balance and SHRIMP ion microprobe results, in: Ringrosevoase, A.J., Humphreys, G.S. (eds.), *Soil Micromorphology: Studies in Management and Genesis*. Developments in Soil Science, 65-81.
- CAO, X. D., WANG, X. R. & ZHAO, G. W. 2000. Assessment of the bioavailability of rare earth elements in soils by chemical fractionation and multiple regression analysis. *Chemosphere*, 40, 23-28.
- CAO, X. D., CHEN, Y., WANG, X. R. & DENG, X. H. 2001. Effects of redox potential and pH value on the release of rare earth elements from soil. *Chemosphere*, 44, 655-661.
- CASPARI, T., BAUMLER, R., NORBU, C., TSHERING, K. & BAILLIE, I. 2006. Geochemical investigation of soils developed in different lithologies in Bhutan, Eastern Himalayas. *Geoderma*, 136, 436-458.
- COPPIN, F., BERGER, G., BAUER, A., CASTET, S. & LOUBET, M. 2002. Sorption of lanthanides on smectite and kaolinite. *Chemical Geology*, 182, 57-68.
- CULLERS, R. L., BARRETT, T., CARLSON, R. & ROBINSON, B. 1987. Rare-earth element and mineralogical changes in holocene soil and stream sediment-a case study in the wet mountains, Colorado, USA. *Chemical Geology*, 63, 275-297.
- DAVRANCHE, M., POURRET, O., GRUAU, G. & DIA, A. 2004. Impact of humate complexation on the adsorption of REE onto Fe oxyhydroxide. *Journal of Colloid and Interface Science*, 277, 271-279.
- DAY, P. R. 1965. Particle fraction standard particle size analysis, Madison, American Society of Agronomy.
- ELDERFIELD, H. & GREAVES, M. J. 1981. Negative cerium anomalies in the Rare-earth element patterns of oceanic ferromanganese nodules. *Earth and Planetary Science Letters*, 55, 163-170.
- FENDORF, S. & FENDORF, M. 1996. Sorption mechanisms of lanthanum on oxide minerals. *Clays and Clay Minerals*, 44, 220-227.
- GOZZARD, J. R., 2007. Geology and landforms of the Perth Region. *Western Australia Geological Survey*, Perth.
- HALL, G. E. M., VAIVE, J. E., BEER, R. & HOASHI, M. 1996. Selective leaches revisited, with emphasis on the amorphous Fe oxyhydroxide phase extraction. *Journal of Geochemical Exploration*, 56, 59-78.
- HARTER, R. D. 1983. Effect of soil-pH on adsorption of lead, copper, zinc, and nickel. *Soil Science Society of America Journal*, 47, 47-51.
- HENDERSON, P. 1984. Rare earth element geochemistry,

continued on page 14

Particle size fractionation and chemical speciation of REE...

continued from page 13

- Amsterdam, Elsevier Science Publishers.
- KEW, G. A. & GILKES, R. J. 2007. Properties of regolith beneath lateritic bauxite in the Darling Range of south Western Australia. *Australian Journal of Soil Research*, 45, 164-181.
- KOEPPEKASTROP, D. & DECARLO, E. H. 1992. Sorption of rare-earth elements from seawater onto synthetic mineral particles-an experimental approach. *Chemical Geology*, 95, 251-263.
- KOEPPEKASTROP, D. & DECARLO, E. H. 1993. Uptake of rare-earth elements from solution by metal-oxides. *Environmental Science & Technology*, 27, 1796-1802.
- LAND, M., OHLANDER, B., INGRI, J. & THUNBERG, J. 1999. Solid speciation and fractionation of rare earth elements in a spodosol profile from northern Sweden as revealed by sequential extraction. *Chemical Geology*, 160, 121-138.
- LAVEUF, C. & CORNU, S. 2009. A review on the potentiality of rare earth elements to trace pedogenetic processes. *Geoderma*, 154, 1-12.
- LJUNG, K., SELINUS, O., OTABBONG, E. & BERGLUND, M. 2006. Metal and arsenic distribution in soil particle sizes relevant to soil ingestion by children. *Applied Geochemistry*, 21, 1613-1624.
- MARKER, A. & DEOLIVEIRA, J. J. 1994. Climatic and morphological control of rare-earth element distribution in weathering mantles on alkaline rocks. *Catena*, 21, 179-193.
- MARSHALL, T.J., 1947. Mechanical composition of soil in relation to field descriptions of texture. Council for Scientific and Industrial Research, Australia.
- MARSHALL, T.J., 2003. Particle-size distribution of soil and the perception of texture. *Australian Journal of Soil Research*, 41, 245-249.
- NEDEL, S., DIDERIKSEN, K., CHRISTIANSEN, B. C., BOVET, N. & STIPP, S. L. S. 2010. Uptake and release of Cerium during Fe-oxide formation and transformation in Fe(II) solutions. *Environmental Science & Technology*, 44, 4493-4498.
- PIASECKI, W. & SVERJENSKY, D. A. 2008. Speciation of adsorbed yttrium and rare earth elements on oxide surfaces. *Geochimica et Cosmochimica Acta*, 72, 3964-3979.
- PRESCOTT, J. A., TAYLOR, J. K. & MARSHALL, T. J., 1934. The relationship between the mechanical composition of the soil and the estimate of texture in the field. Transaction 1st Commission International Society of Soil Science.
- QUINN, K. A., BYRNE, R. H. & SCHIJF, J. 2006. Sorption of yttrium and rare earth elements by amorphous ferric hydroxide: Influence of solution complexation with carbonate. *Geochimica et Cosmochimica Acta*, 70, 4151-4165.
- RAYMENT, G. E. & HIGGINSON, F. R. 1992. Australian laboratory handbook of soil and water chemical methods. Melbourne, Inkata Press.
- SADLEIR, S. B. & GILKES, R. J. 1976. Development of bauxite in relation to parent material near Jarrahdale, Western Australia. *Journal of the Geological Society of Australia*, 23, 333-344.
- SONKE, J. E. & SALTERS, V. J. M. 2006. Lanthanide-humic substances complexation. I. Experimental evidence for a lanthanide contraction effect. *Geochimica Et Cosmochimica Acta*, 70, 1495-1506.
- SUTHERLAND, R. A. 2003. Lead in grain size fractions of road-deposited sediment. *Environmental Pollution*, 121, 229-237.
- TARI, G., BOBOS, I., GOMES, C. S. F. & FERREIRA, J. M. F. 1999. Modification of surface charge properties during kaolinite to halloysite-7Å transformation. *Journal of Colloid and Interface Science*, 210, 360-366.
- WANG, X.-S., QIN, Y. & CHEN, Y.-K. 2006. Heavy metals in urban roadside soils, part 1: effect of particle size fractions on heavy metals partitioning. *Environmental Geology*, 50, 1061-1066.
- WOOD, S. A. 1993. The aqueous geochemistry of the rare-earth elements: critical stability constants for complexes with simple carboxylic acids at 25°C and 1 bar and their application to nuclear waste management. *Engineering Geology*, 34, 229-259.

Xin Du*, Andrew W. Rate, M.A. Mary Gee

School of Earth and Environment

University of Western Australia,

Crawley, 6009, WA, Australia

Email: dux01@student.uwa.edu.au

*School of Environmental Studies

China University of Geosciences

430074, Wuhan, China

Appendix 1: Detection limits for elements determined by EMPA: a) fluorocarbonate; b) florencite; c) rhabdophane; d) ilmenite.

Sample Detection limit (wt%)

Sample	Si	Ti	Pb	Th	U	Al	Y	La	Ce	Pr	Nd	Sm	Eu	Gd	Dy	Yb	Lu	Fe	Mg	Ca	P	S	F	
a	0.01	0.01	0.02	0.02	0.02	0.01	0.02	0.04	0.04	0.03	0.04	0.02	0.01	0.02	0.02	0.02	0.02	0.01	0.02	0.01	0.01	0.01	0.01	0.07
b	0.01	0.01	0.02	0.01	0.01	0.01	0.01	0.04	0.03	0.03	0.03	0.02	0.01	0.02	0.02	0.01	0.02	0.01	0.01	0.01	0.01	0.01	0.01	0.10
c	0.01	0.01	0.02	0.02	0.02	0.01	0.02	0.04	0.04	0.03	0.04	0.02	0.01	0.02	0.02	0.01	0.02	0.01	0.02	0.01	0.01	0.01	0.01	0.08
d	0.01	0.01	0.01	0.01	0.01	0.01	0.01	0.03	0.03	0.04	0.03	0.05	0.01	0.02	0.04	0.01	0.02	0.01	0.01	0.01	0.01	0.01	0.01	0.12

